

Dynamical Instabilities in Extrasolar Planetary Systems Containing Two Giant Planets

Eric B. Ford¹, Marketa Havlickova², and Frederic A. Rasio³

Department of Physics, MIT, Cambridge, MA 02139

Received _____; accepted _____

submitted to Icarus, October 10, 2000

¹Present address: Department of Astrophysical Sciences, Princeton University, Princeton, NJ 08544; eford@princeton.edu.

²Also Department of Mathematics, MIT; mikiavl@mit.edu

³Sloan Research Fellow; rasio@mit.edu.

ABSTRACT

Instabilities and strong dynamical interactions between several giant planets have been proposed as a possible explanation for the surprising orbital properties of extrasolar planetary systems. In particular, dynamical instabilities would seem to provide a natural mechanism for producing the highly eccentric orbits seen in many systems. Here we present results from a new set of numerical integrations for the dynamical evolution of planetary systems containing two identical giant planets in nearly circular orbits very close to the dynamical stability limit. We determine the statistical properties of the three main types of systems resulting from the development of an instability: systems containing one planet, following either a collision between the two initial planets, or the ejection of one of them to infinity, and systems containing two planets in a new, quasi-stable configuration. We discuss the implications of our results for the formation and evolution of observed extrasolar planetary systems. We conclude that the distributions of eccentricities and semimajor axes for observed systems cannot be explained easily by invoking dynamical interactions between two planets initially on circular orbits. While highly eccentric orbits can be produced naturally by these interactions, collisions between the two planets, which occur frequently in the range of observed semimajor axes, would result in many more nearly circular orbits than in the observed sample.

Subject headings: Planets and Satellites: General — Solar System: General — Stars: Planetary Systems

1. Introduction and Motivation

The existence of planetary systems around other stars is now well established. For several years already, we have known many more planets outside than inside our own Solar System (currently ~ 50 , including planets around radio pulsars). Several groups with ongoing radial-velocity surveys have reported many unambiguous detections of Jupiter-mass planets around nearby solar-like stars (for recent reviews and updates, see Marcy and Butler 1998, 2000; Hatzes *et al.* 2000; Korzennik *et al.* 2000; Perryman 2000; Vogt *et al.* 2000; Santos *et al.* 2000). Astrometry can sometimes help constrain the parameters of the wider systems (e.g., Mazeh *et al.* 1999) and other, newer techniques such as gravitational microlensing (Gaudi *et al.* 2000) and space interferometry (Fridlund 1999) are making rapid progress. Some of the most exciting recent developments include the detections of planetary transits in HD 209458 (Charbonneau *et al.* 2000; Henry *et al.* 2000) and two sub-Saturn-mass candidates around HD 16141 and HD 46375 (Marcy *et al.* 2000).

The long-term stability of the Solar System, in spite of its chaotic nature (see, e.g., Duncan and Quinn 1993), may have been necessary for the development of intelligent life. However, it may also be very *atypical*, and may in fact require very special conditions during the early stages of planet formation. In particular, the existence of a single dominant massive planet in our Solar System (Jupiter), although perhaps essential for long-term dynamical stability, may not be typical of planetary systems that form around other stars. In fact, current theoretical models for the formation of giant planets by accretion of gas from the nebula onto a rocky core, combined with observed mass distributions of protoplanetary disks (e.g., Beckwith and Sargent 1996) suggest that many planetary systems could form initially with 2–3 Jupiters. In a sufficiently massive protoplanetary disk ($\gtrsim 0.01M_{\odot}$), disk instabilities may also lead naturally to the formation of several giant planets (Armitage and Hansen 1999; Boss 1998). However, one should be careful not to rely solely on theoretical

models for planet formation that, for many decades, have been based on only the Solar System for guidance. What the newly detected systems (see Fig. 1) clearly tell us is that there exists a much greater variety of other planetary systems than theorists had ever imagined. Some of the unexpected properties of these systems (e.g., highly eccentric orbits) suggest that, unlike our Solar System, they may well have been affected by dynamical instabilities (Rasio and Ford 1996; Weidenschilling and Marzari 1996; Lin and Ida 1997).

In a system containing two or more Jupiter-like planets of comparable masses the possibility exists that a dynamical instability will develop, leading to strong gravitational interactions or collisions between the planets (Gladman 1993, Chambers *et al.* 1996). Here we will use numerical integrations of the orbital dynamics to explore the consequences of such dynamical instabilities. Based on a preliminary set of calculations for systems containing two identical giant planets (Rasio and Ford 1996) we expect a frequent outcome of these instabilities to be a physical collision between two giant planets. Very little mass is lost in such a collision, and the result is therefore a more massive giant planet in a slightly more eccentric orbit. However, in many cases, the interaction can also lead to the ejection of one planet to a larger distance while the other is left in a slightly smaller, highly eccentric orbit. If the inner eccentric orbit has a short enough pericenter distance (distance of closest approach to the star), it may later circularize through tidal dissipation, leaving a Jupiter-type planet in a very tight circular orbit around the star, with an orbital period typically of order a few days. Indeed, all the recently detected planets around nearby stars are Jupiter-mass objects in very tight circular orbits, or in wider eccentric orbits (Fig. 1). The standard model for planet formation in our Solar System (see, e.g., Lissauer 1993) is incapable of explaining them. According to this standard model, planetary orbits should be nearly circular, and giant planets can only form at large distances ($\gtrsim 1$ AU) from the central star, where the temperature in the protostellar nebula is low enough for icy materials to condense (Boss 1995, 1996).

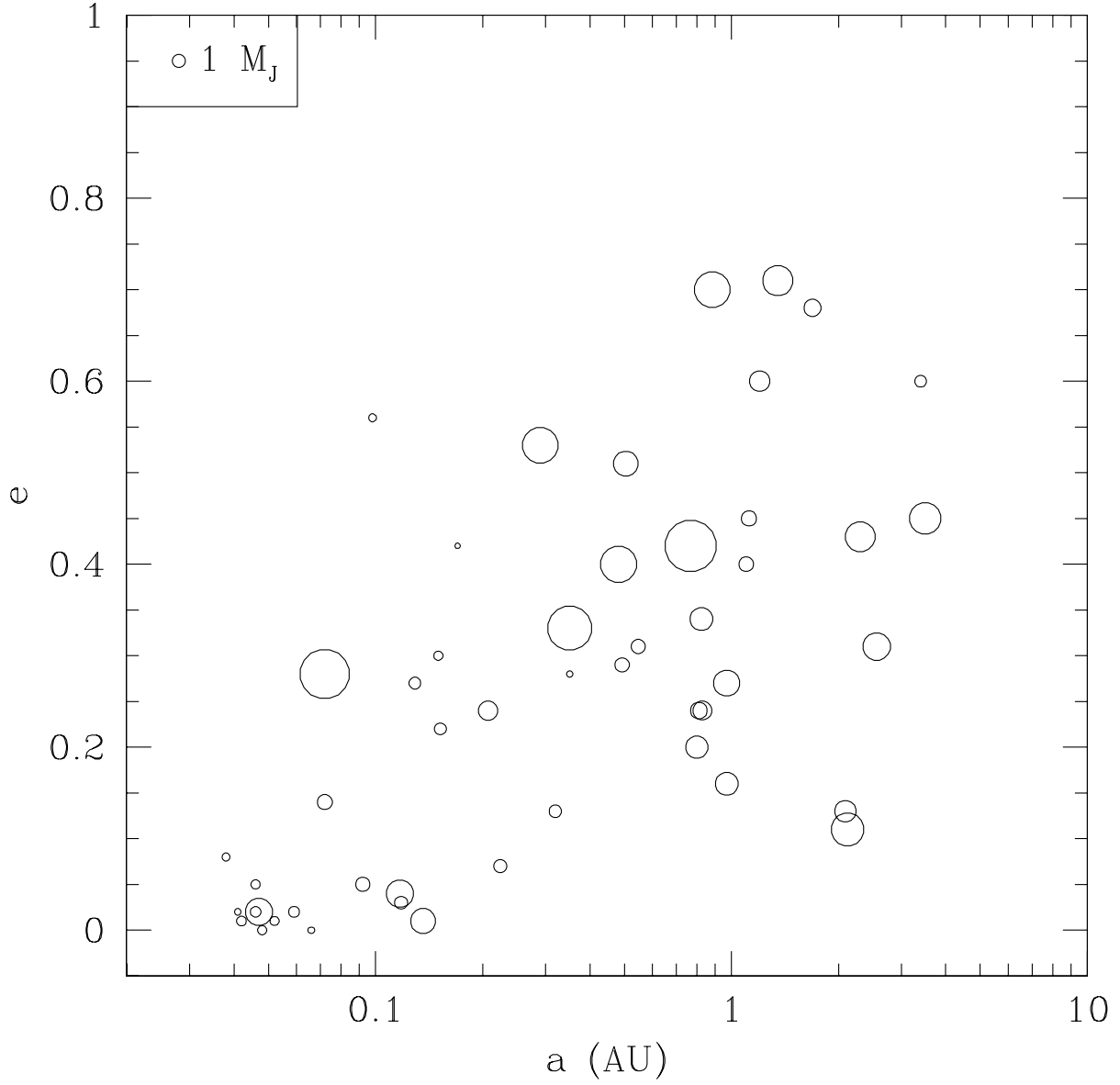


Fig. 1.— Semimajor axes and eccentricities of all presently known radial-velocity planetary candidates with $m \sin i < 13M_J$ (M_J is the mass of Jupiter). The area of each open dot is proportional to the value of $m \sin i$ for that object. One group of planets has $a \lesssim 0.07$ AU and nearly circular orbits, while the other, with $a \gtrsim 0.07$ AU, contains many highly eccentric orbits. The data shown here include all planets discovered up to and including the one in ϵ Eri (see Hatzes *et al.* 2000 and references therein). Values of $m \sin i$, a and e for 50 planets were taken from the table compiled by Marcy *et al.* at <http://exoplanets.org/> as of Oct 28, 2000.

There are many ways for dynamical instabilities to develop in a protoplanetary system. The simplest scenario, that we will be assuming here, is that two nearly identical giant planets had initially formed (in the conventional way) at a large distance from the central star, and later interacted dynamically (Rasio and Ford 1996). This could happen because their orbital radii evolved secularly at different rates (significant orbital migration is thought to have occurred in the outer Solar System; see Goldreich and Tremaine 1980, Malhotra 1995), bringing them closer together, or because the masses increased as the planets accreted their gaseous envelopes (Lissauer 1993), or both (see Kley 2000, who shows that a system of two identical giant planets still embedded in a protoplanetary disk generically evolves toward a dynamical instability). The dynamical instability leads eventually to orbit crossing and strong gravitational interactions between the two planets (Gladman 1993).

Other formation mechanisms have been proposed for the 51-Peg-type planets (in very tight circular orbits with orbital periods $\sim 3 - 5$ d). If these planets had formed, like our own Jupiter, at a large distance from the central star, some angular-momentum-loss mechanism must have brought them in. A *slow migration* mechanism, such as friction in the protostellar nebula or interaction with a protoplanetary disk, would tend to increase rapidly with decreasing separation. The dissipation would have had to switch off at a critical moment for the planets to end up so close to the star without being disrupted. Although there exist mechanisms that can provide a barrier at some very short distance from the star (Lin *et al.* 1996; Murray *et al.* 1998; Trilling *et al.* 1998), this always seems to require some fine tuning of the parameters or extreme conditions such as a very massive disk (Murray *et al.* 1998; Rasio *et al.* 1996). Alternatively, direct *in situ* formation of all 51-Peg-type planets by accretion onto a solid core may also be possible under some conditions (Bodenheimer *et al.* 2000).

Alternative mechanisms for inducing a large eccentricity in a planetary orbit include

the gravitational perturbation by a distant binary stellar companion (Holman *et al.* 1997; Mazeh *et al.* 1997) and dynamical interactions with a gaseous protoplanetary disk (Papaloizou 2000) or with a disk of planetesimals (Murray *et al.* 1998). Perturbations of planetary orbits in a binary star system are well understood theoretically (see, e.g., Ford *et al.* 2000; Innanen *et al.* 1997) and can lead to arbitrarily large eccentricities provided that the relative inclination is large enough and the binary companion is not too far from the planet. While interactions with a disk typically *damp* orbital eccentricities, they may in some special situations lead to modest eccentricity growth. However, within our limited current theoretical understanding of these processes (see, e.g., Nelson *et al.* 2000), it appears unlikely that they would be able to produce eccentricities as large as those observed for many Jupiter-mass objects (with measured eccentricities up to $e \simeq 0.7$; see Fig. 1).

The strongest observational evidence to date that extrasolar planetary systems may be affected by dynamical instabilities is provided by the recent detection of two giant planets in wide eccentric orbits around ν And (Butler *et al.* 1999). These are in addition to the previously discovered 51-Peg-type planet, in a 4.6-day, nearly circular orbit around the star. The presence of one or more additional giant planets *in wider eccentric orbits* in the 51-Peg-type systems is a basic theoretical prediction of our mechanism (see Rasio and Ford 1996), since at least one other planet of comparable mass must have been present to trigger an instability. Moreover, the two outer orbits in ν And are tightly coupled (ratio of semimajor axes $\simeq 1/3$) and the system is still very close to the edge of dynamical stability (numerical integrations indicate that it may in fact be unstable on timescales $\sim 10^6 - 10^7$ yr depending on the precise values of the masses and orbital parameters; see Rivera and Lissauer 2000). This provides further evidence that the present configuration resulted from the evolution of the progenitor planetary system through a phase of violent dynamical instability. Indeed, systems of multiple planets that become unstable tend to evolve first through a violent phase where energy and angular momentum are quickly redistributed,

followed by a much more gradual settling into a more stable configuration that remains very close to the stability edge (Chambers *et al.* 1996).

Additional support for a scenario based on dynamical instabilities comes from the latest detection, around the nearby K2 V star ϵ Eri: a planet with mass $m \sin i = 0.86 M_J$, a long orbital period $P = 6.9$ yr ($a \simeq 3.3$ AU), and a large eccentricity $e \simeq 0.6$ (Hatzes *et al.* 2000). The star is not in a binary system and, at this large orbital separation, the planet is unlikely to have had a significant interaction with a protoplanetary disk (which would also have produced significant inward migration). This clearly leaves dynamical interaction with another giant planet (which was likely ejected from the system) as the most natural explanation.

While our study will concentrate on the systematic study of a system containing two giant planets, other groups have performed small numbers of exploratory calculations to determine the consequences of dynamical instabilities in systems containing three planets or more. Weidenschilling and Marzari (1996) have published results for the case of three planets, while Lin and Ida (1997) presented results for systems containing up to 9 planets. With many planets, successive collisions and mergers can lead to the formation of a fairly massive ($\gtrsim 10 M_J$) object in a wide, eccentric orbit. We feel that it is important to first understand fully the case of two planets. One important advantage of the two-planet case is that the dynamical stability boundary is very sharply defined, and its location known analytically (Gladman 1993). Therefore, the initial value for the ratio of semimajor axes a_2/a_1 must be varied only in a very narrow range (right around the stability boundary) for each case. In contrast, for three or more planets, the stability boundary is not well defined (Chambers *et al.* 1996), and a much wider range of semimajor axis ratios would have to be explored. In addition, if the instability is triggered by the increase in the mass of one planet as it accretes its gaseous envelope, we would expect that it would naturally tend

to involve only two giant planets, since it appears extremely unlikely that more than two planets would be going through the accretion process at precisely the same time. Indeed a time difference $\gtrsim 10^6$ yr between the formation of the different giant planets would be expected from the standard scenario (Lissauer 1993).

2. Methods and Assumptions

Our numerical integrations were performed for a system containing two identical planets, with a mass ratio $m/M = 10^{-3}$, where m is the planetary mass and M is the mass of the central star (This corresponds to $m \simeq 1 M_J$ for $M = 1 M_\odot$). For this system, the dynamical stability limit (for circular, coplanar initial orbits) corresponds to $\alpha \equiv a_1/a_2 = 0.769$, where a_1 and a_2 are the semimajor axes of the two planets (Gladman 1993). Our simulations were started with α randomly chosen in the range from 0.769 to 0.781 (See Sec. 3 for a justification of this range). The initial eccentricities were distributed uniformly in the range from 0 to 0.01, and the initial relative inclination in the range from 0 to 5° . All remaining angles (longitudes and phases) were randomly chosen between 0 and 2π . Throughout this paper we quote numerical results in units such that $G = a_1 = M = 1$. In these units, the initial orbital period of the inner planet is $P_1 \simeq 2\pi$.

The orbital integrations were performed using a modified version of SWIFT, a standard software package for orbital dynamics developed by Levison and Duncan (1994). The package features several integrators, including a Bulirsch-Stoer (BS) integrator and a mixed variable symplectic integrator (MVS).

The BS integrator directly solves the second-order differential equations of motion. For this work we have modified the BS integrator to allow for regularization: whenever the outermost planet is sufficiently distant from the inner planet(s) and the central star,

the outer planet is analytically advanced in its orbit and the motion of the inner planets is integrated separately for the time necessary to bring the outer planet back within the specified distance of other planets. The direct integration of the dynamical equations then continues according to the original BS integrator. For the case of two planets, this leads to a phase of the evolution where both planets are following unperturbed Keplerian orbits. In our specific case, whenever $r_2/r_{\text{apo},1} > 100$, we switch to analytic Keplerian orbits.

The MVS integrator exactly solves an approximation of the system’s Hamiltonian (Wisdom and Holman 1991, 1992). While the MVS integrator is nearly an order of magnitude faster, it cannot handle close encounters between the planets. Therefore we only use the MVS integrator to determine the location of the stability boundary, and to integrate all systems up to the first strong interaction. Then the regularized BS integrator takes over to follow the evolution of unstable systems.

Throughout the integrations, close encounters between any two bodies were logged, allowing us to present results for any values of the planetary radii using a single set of orbital integrations. However, the integration was stopped if the two planets collided with an assumed minimum radius $R_{\text{min}}/a_1 = 0.1 R_{\text{J}}/5 \text{ AU} = 0.95 \times 10^{-5}$ (where $R_{\text{J}} = 7 \times 10^9 \text{ cm}$ is Jupiter’s radius), or if either planet came to within a distance $r_{\text{min}}/a_1 = 10 R_{\odot}/1 \text{ AU} = 0.01$ of the star (see below).

The BS integrations were performed using an accuracy parameter of 10^{-12} , which is used to determine each stepsize. All integrations conserved total energy and angular momentum within 10^{-4} , although for most runs energy and angular momentum were conserved to 10^{-6} . The computations were performed on the SGI/Cray Origin2000 supercomputers at the National Center for Supercomputing Applications and at Boston University, and on the Condor cluster of Sun workstations operated by the University of Wisconsin. The results presented in this paper are based on $\sim 10^3$ numerical integrations

all performed for systems with initial parameters in the ranges specified above⁴. Each run was terminated when one of the following four conditions was encountered: (i) one of the two planets became unbound (which we defined as having positive energy, a positive radial velocity, and being at least 100 times as distant from the star as the other planet); (ii) a collision between the two planets occurred assuming $R = R_{\min}$; (iii) a close encounter occurred between a planet and the star (defined by having a planet come within r_{\min} of the star); (iv) the integration time reached $t_{\max} = 10^7$ (corresponding to about $1.6 \times 10^6 P_1$). The percentages of runs that terminated according to each condition were approximately: (i) 50%; (ii) 5%; (iii) $< 1\%$; (iv) 45%. The total CPU time required for this study was about 12,000 hours, corresponding to an average of about 12 CPU hours per run.

Since collisions of a planet with the star seem to occur so rarely, only three types of outcomes will be discussed in the rest of the paper. These three types will be referred to as “collisions,” meaning a collision between the two planets, “ejections,” meaning that one planet was ejected to infinity, and “two planets,” meaning that two bound planets remained in a (possibly new) dynamically stable configuration.

3. Results

For a study of this type to be meaningful, it is crucial to establish that the integration time is long enough for the system to have reached its true final configuration. Fig. 2 shows the branching ratios for the three types of outcomes as a function of integration time, for an assumed planetary radius $R/a_1 = 3 R_J/5 \text{ AU} = 2.9 \times 10^{-4}$. While collisions nearly always

⁴The initial parameters used in the preliminary study by Rasio and Ford (1996) were slightly different, and the shorter numerical integrations did not provide a good basis for a statistical analysis of the final properties of unstable systems.

occur soon after the development of the instability (within $t \sim 10^5$, nearly independent of the planetary radius, see Fig. 3), ejections can take a much longer time. This is because the exchange of energy between the two planets typically takes place through a large number of very weak interactions, rather than just one strong interaction⁵ (see Fig. 4). We see in Fig. 2 that for integration times $t_{\text{int}} \gtrsim 6 \times 10^6$, the branching ratios become nearly constant, as desired. All results shown in the rest of this section correspond to an integration time $t_{\text{max}} = 10^7$. Fig. 5 shows the evolution of a typical system for which our numerical integration was terminated at $t = t_{\text{max}}$ while the two planets were still in a bound configuration, even though a strong dynamical instability had clearly developed.

We have also checked that the distributions of orbital parameters determined for each type of final outcome are independent of the precise values of the initial parameters used within the narrow ranges considered. For example, we see no statistically significant variation in the distributions of final orbital parameters measured for systems starting in different sub-ranges of values for α . This suggests that the properties of systems affected by an instability will be largely independent of the particular mechanism triggering the instability (which may determine the exact location of the system near the stability boundary). Similarly, we have verified that our results are independent of the precise range of small eccentricities and inclinations assumed in constructing the initial conditions. However, we find that, as expected, the *branching ratios* for different types of outcomes do show a significant dependence on α (Fig. 6). Indeed, for systems very near the edge of stability, we expect that the branching ratio for retaining two planets in a stable configuration should approach unity, while it should go to zero further away into the unstable region. From Fig. 6 we see that the transition region extends from the theoretical

⁵For this reason also, the simple arguments presented by Katz (1997), assuming a single strong interaction between two planets, are irrelevant for real systems.

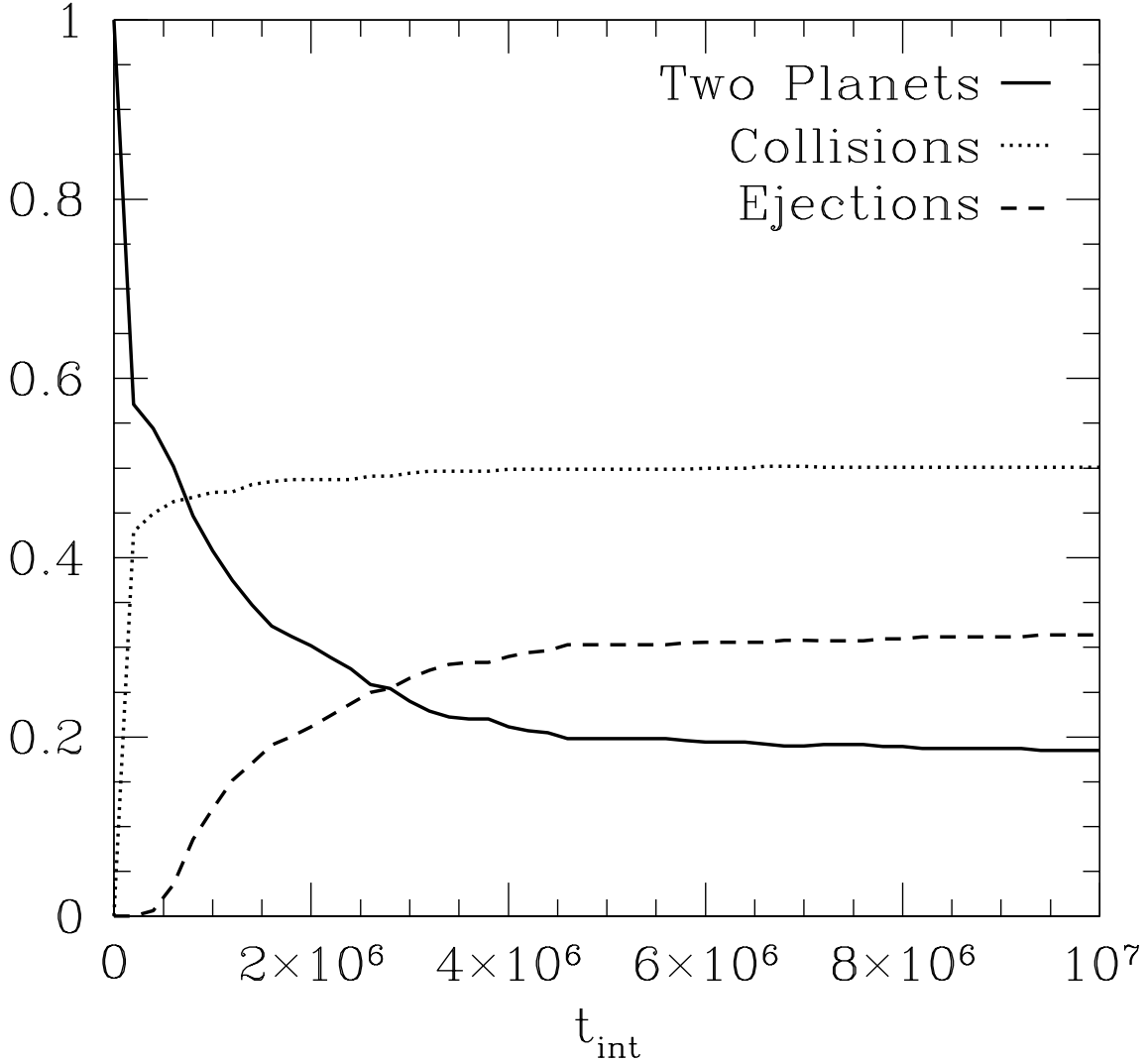


Fig. 2.— Branching ratios of various outcomes as a function of maximum integration time (here and throughout this paper units are defined by $G = a_1 = M = 1$, where a_1 is the initial semimajor axis of the inner planet and M is the mass of the central star). The dashed line corresponds to the ejection of one planet from the system, the dotted line to a collision between the two planets (here assuming that the planetary radius is given by $R/a_1 = 3 R_J/5 \text{ AU} = 2.9 \times 10^{-4}$, and the solid line to cases where both planets remain in a bound configuration. The branching ratios are well determined for $t_{\text{int}} = t_{\text{max}} = 10^7$, used in the rest of this paper.

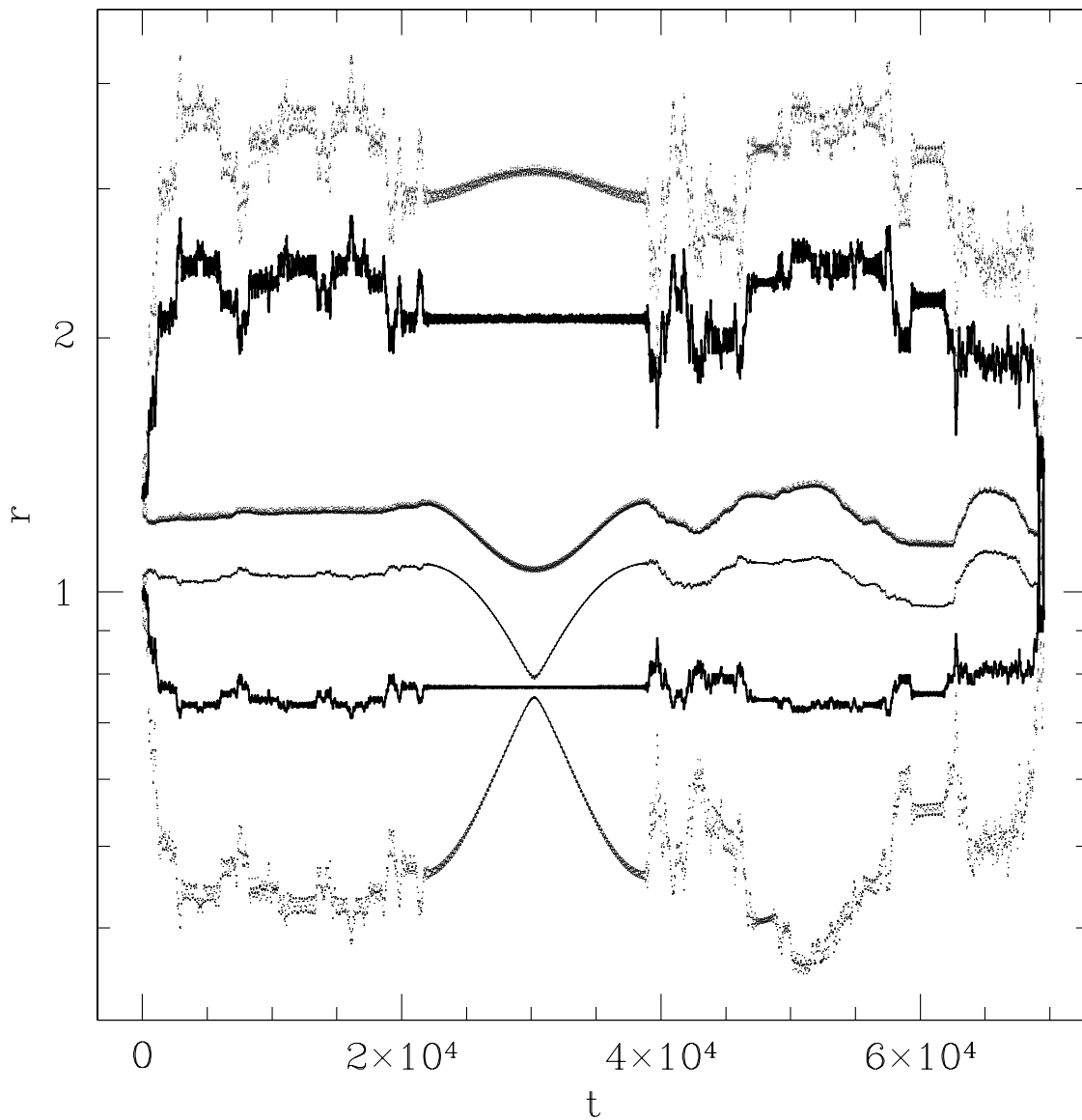


Fig. 3.— Typical evolution of a system resulting in a collision between the two planets (at far right). The two solid lines show the osculating semimajor axes of the two planets. The dotted lines show the osculating pericenter and apocenter distances for each of the two planets.

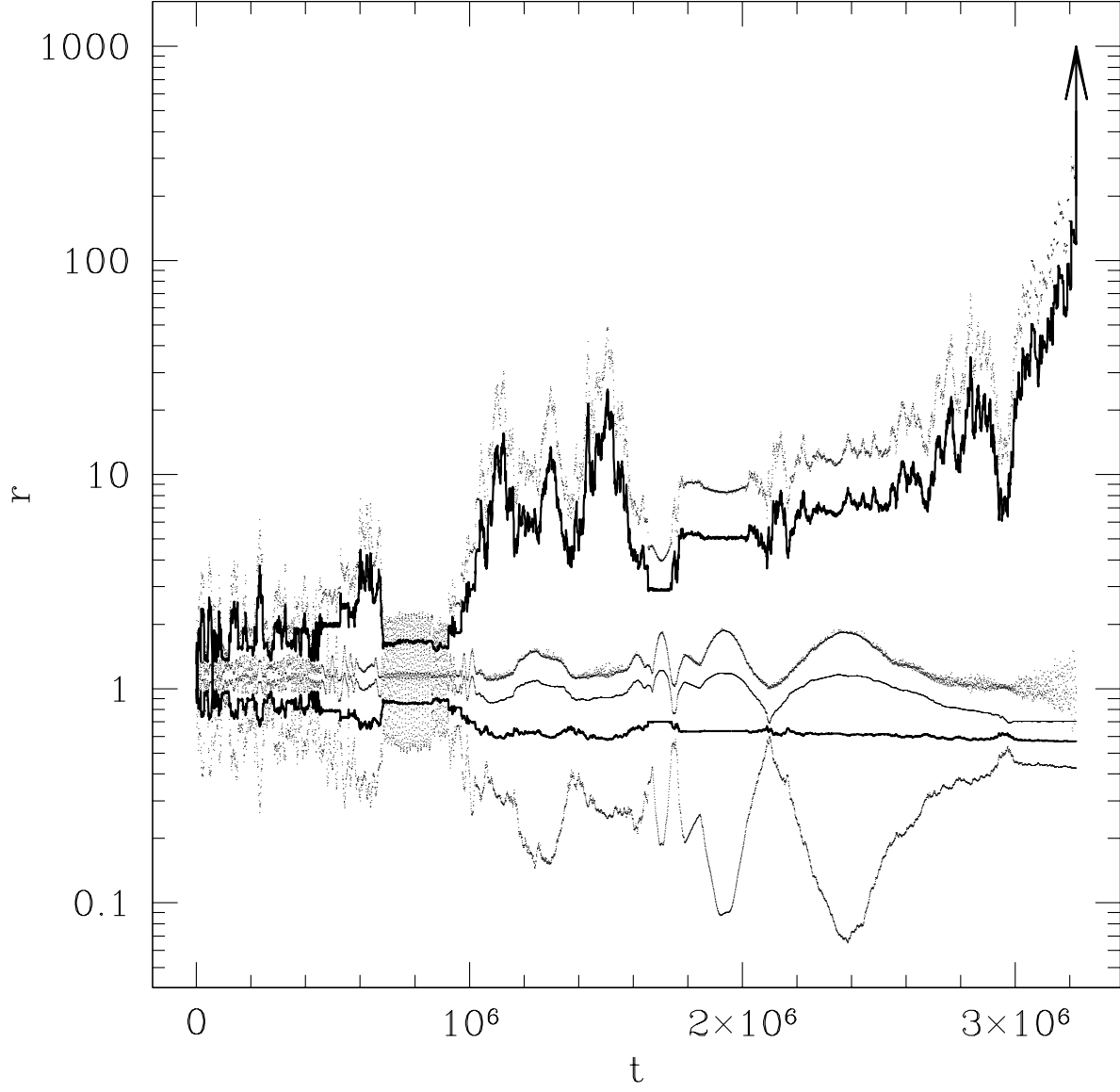


Fig. 4.— Typical evolution of a system resulting in one planet being ejected to infinity (at arrow). Conventions are as in Fig. 3.

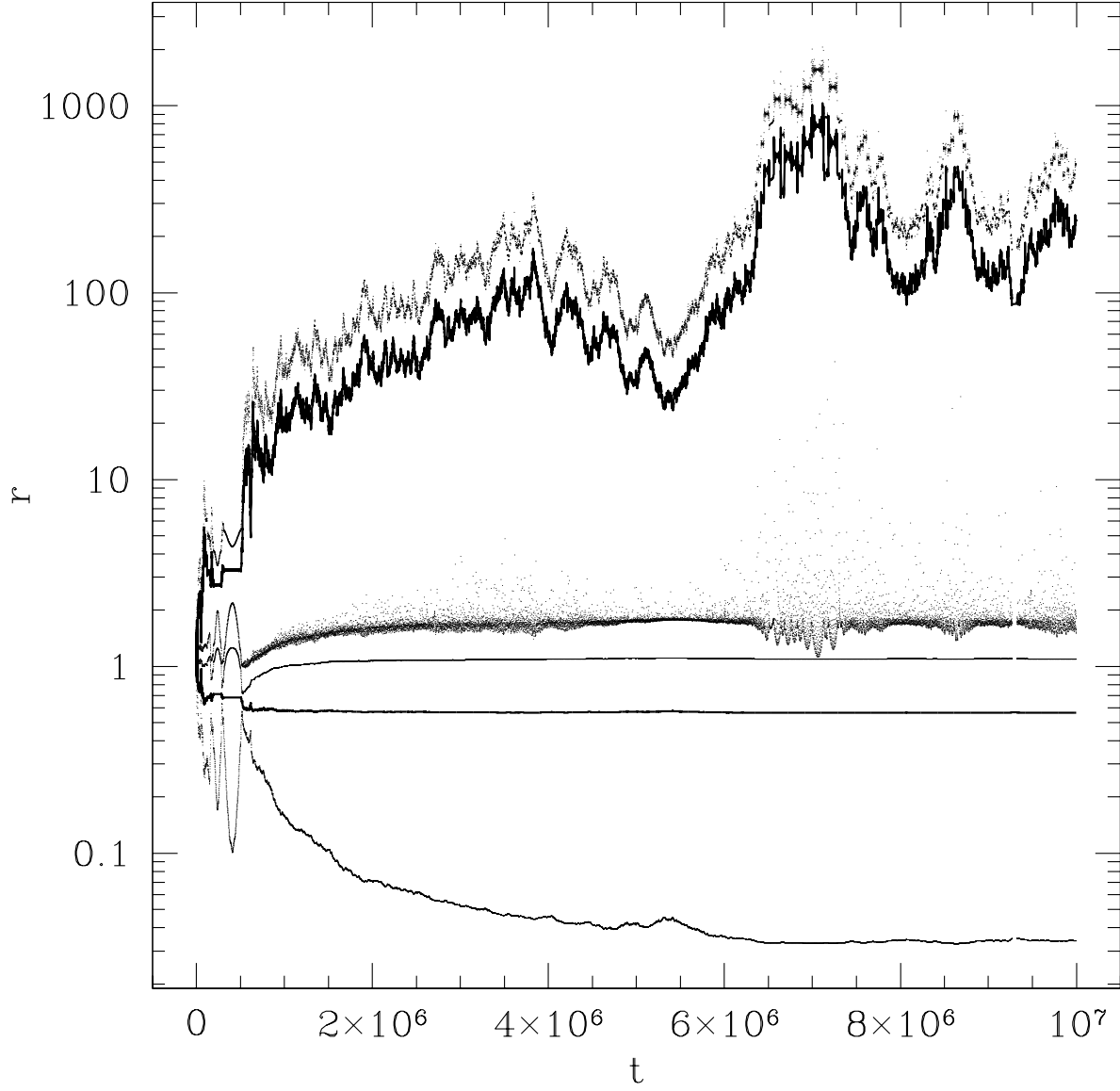


Fig. 5.— Typical evolution of a system that retains both planets following a period of strong dynamical perturbations. Here the two planets are still on bound orbits at the end of the integration, $t = t_{\text{max}} = 10^7$. Conventions are as in Fig. 3.

stability edge at $\alpha^{-1} = a_2/a_1 = 1.3$ (all systems with $a_2/a_1 > 1.3$ must be stable; see Gladman 1993) down to $\alpha^{-1} = a_2/a_1 = 1.28$, where the probability of retaining two planets in a stable configuration goes to nearly zero. Systems entering the unstable region *slowly* (i.e., on a timescale long compared to the typical growth time of dynamical instabilities, $t_{\text{dyn}} \sim 10^4 - 10^5$ yr) will populate the entire range of initial values of α shown in Fig. 6 (justifying our choice of this range). Systems entering the unstable region more rapidly may "overshoot" our range of initial values for α . To model such a rapid evolution correctly would require the inclusion of additional forces (e.g., from hydrodynamics) and is beyond the scope of this paper.

The initial values of the planetary radii can also affect significantly the outcome of a dynamical instability (Fig. 7). We clearly expect larger planets to collide more often, but Fig. 7 reveals that the fraction ejected is only slightly reduced as the planetary radius increases. Instead, as the radius increases, the branching ratio for collisions increases mainly at the expense of the branching ratio for retaining two planets. This is again a consequence of the mechanism for ejections, which proceed through a large number of distant, weak encounters between the two planets. Since the radius of a giant planet depends extremely weakly on its mass, most of the variation in R/a_1 for different planetary systems will come from the initial semimajor axis a_1 . For $R = 1 R_J$, collisions will be very rare in a system with $a_1 = 5$ AU, but they will occur for over 40% of unstable systems with $a_1 = 1$ AU. Note that the radius of a newly formed giant planet can be significantly larger than its radius today (see, e.g., Burrows *et al.* 1997). For Jupiter, the initial radius may have been as large as $\sim 2 R_J$, implying that even for a system with $a_1 = 5$ AU collisions may be significant.

Collisions leave a single, larger planet in orbit around the star. The energy in the center-of-mass frame of the two planets is always much smaller than the binding energy of a giant planet (see Appendix). As a consequence, collisions between giant planets

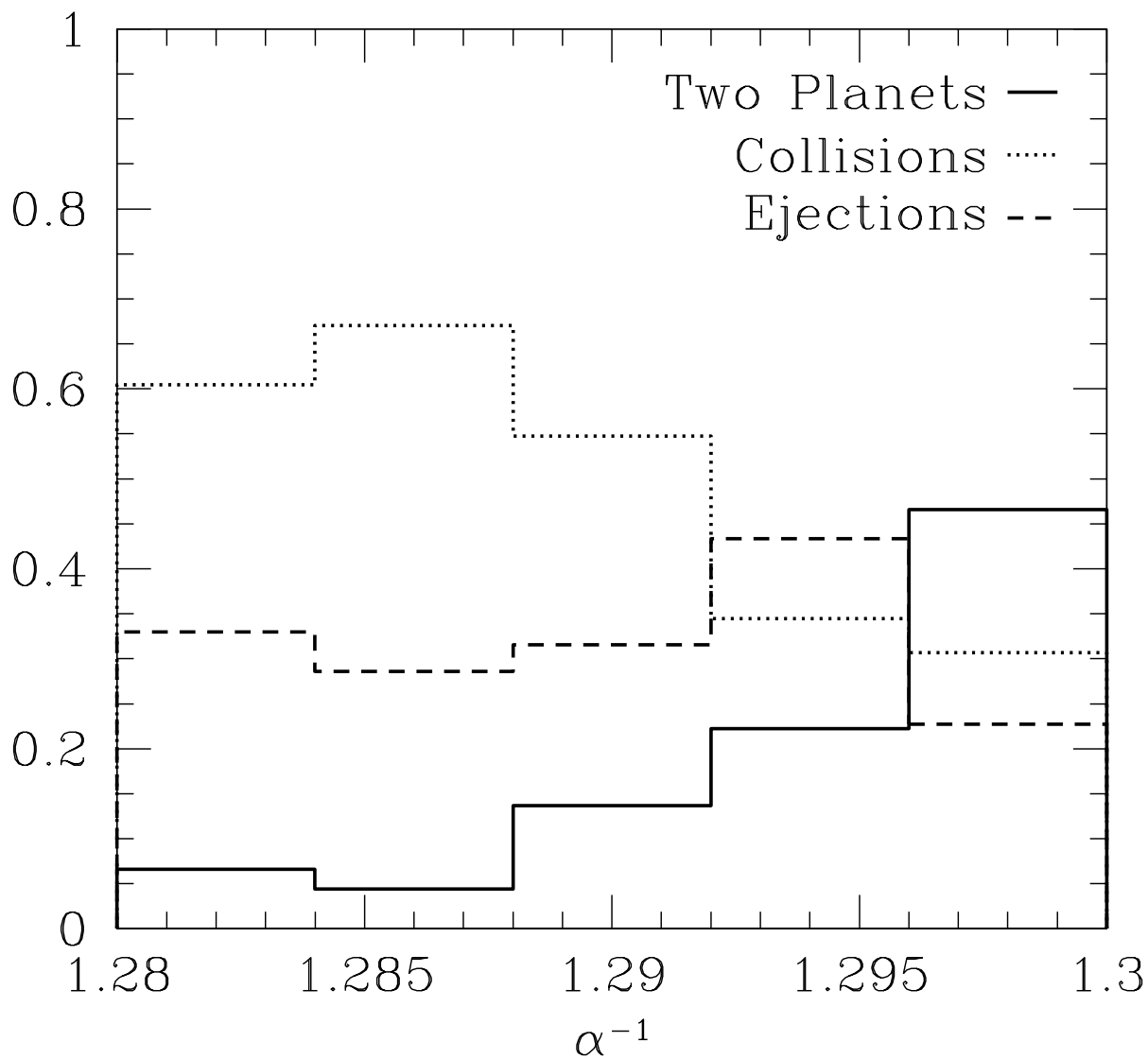


Fig. 6.— Branching ratios of different outcomes measured for different ranges of values of $\alpha^{-1} = a_2/a_1$ (the initial ratio of semimajor axes). Conventions are as in Fig. 2. See text for discussion.

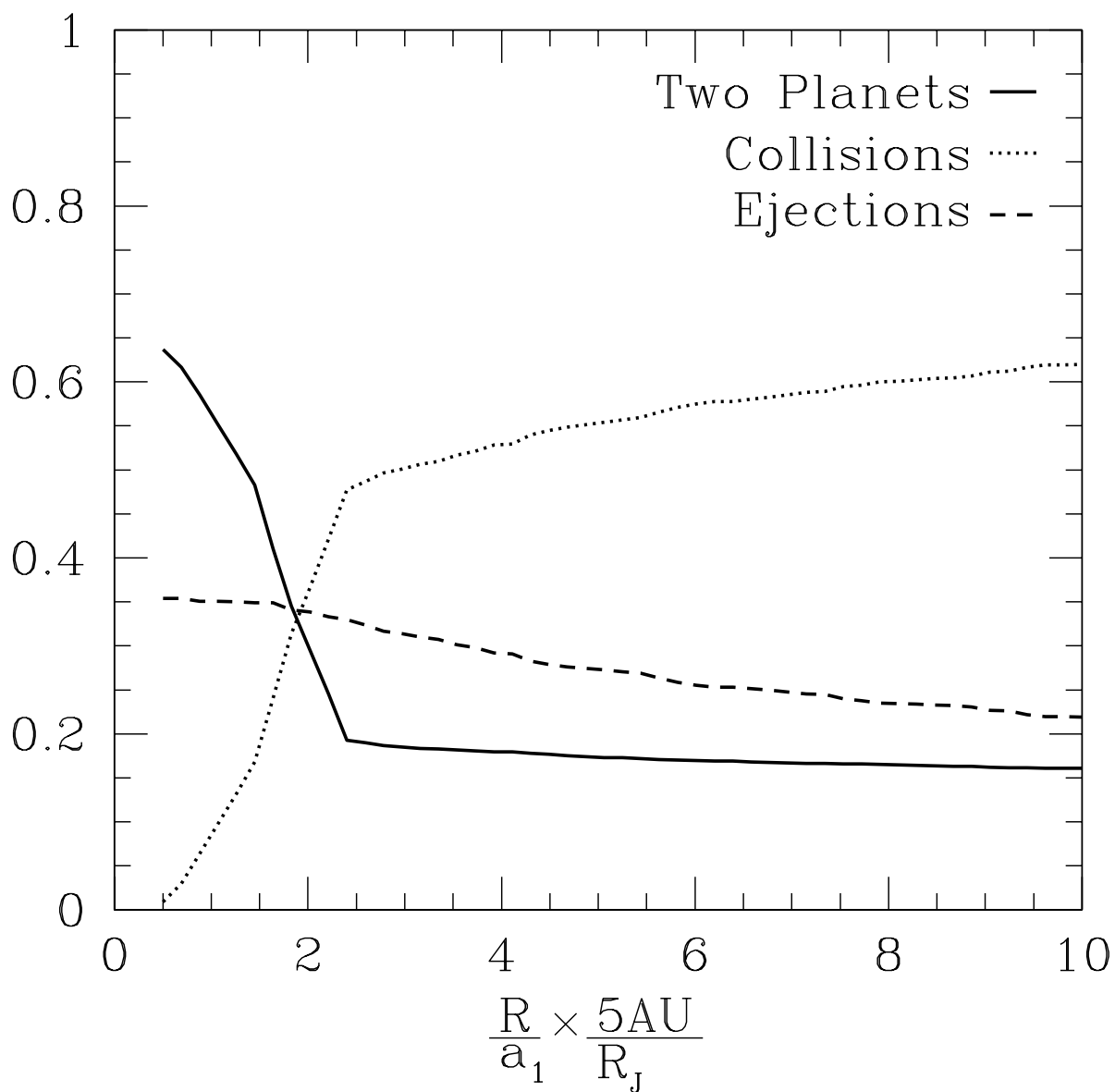


Fig. 7.— Branching ratios for various outcomes as a function of planetary radius R . Conventions are as in Fig. 2. Note how the most probable outcome makes a sharp transition to favor collisions as the planetary radius increases or the semimajor axis decreases.

resemble parabolic collisions between low-mass main-sequence stars in globular clusters. Hydrodynamic calculations show that, as expected from simple energetic arguments, these collisions produce very little mass loss (typically $\lesssim 5\%$; see, e.g., Lombardi *et al.* 1996). Therefore, to a very good approximation, we can model the collisions as completely inelastic and assume that the two giant planets simply merge together while conserving total momentum and mass. Under this assumption, we have calculated the distributions of orbital parameters for the collision products (Fig. 8). The final semimajor axis lies typically just inside the average of the two initial semimajor axes. Eccentricities and inclinations remain very small. These results are consistent with expectations from elementary analytic arguments based on our assumptions (see Appendix).

We now turn to those cases where one planet is ejected from the system. The distributions of orbital elements for the remaining planet are shown in Fig. 9 (we do not distinguish between ejecting what was initially the inner vs outer planet; the outer planet is ejected most often). The escaping planet typically leaves the system with a very small (positive) energy, and the final semimajor axis of the remaining planet is therefore set by energy conservation at a value very near $a_{\text{final}} \simeq a_1 a_2 / (a_1 + a_2) \simeq 0.56$ in our units (See Appendix). However, the escaping planet does carry away significant angular momentum (Fig. 10). As a result, the distribution of final eccentricities is much broader: about 90% of the remaining planets have eccentricities in the range $e_{\text{final}} \simeq 0.4 - 0.8$, with a median value around 0.6. Some planets develop very large eccentricities. Of great potential importance are the few percent of systems with very small pericenter distances ($r_{\text{p,final}} \lesssim 0.1$), which may later become tidally circularized, especially if the central star is still on the pre-main-sequence. Inclinations of remaining planets following an ejection generally remain small, with about 90% of the orbits having $i_{\text{final}} < 10^\circ$.

In two of our numerical integrations ($\ll 1\%$) one planet came extremely close to the

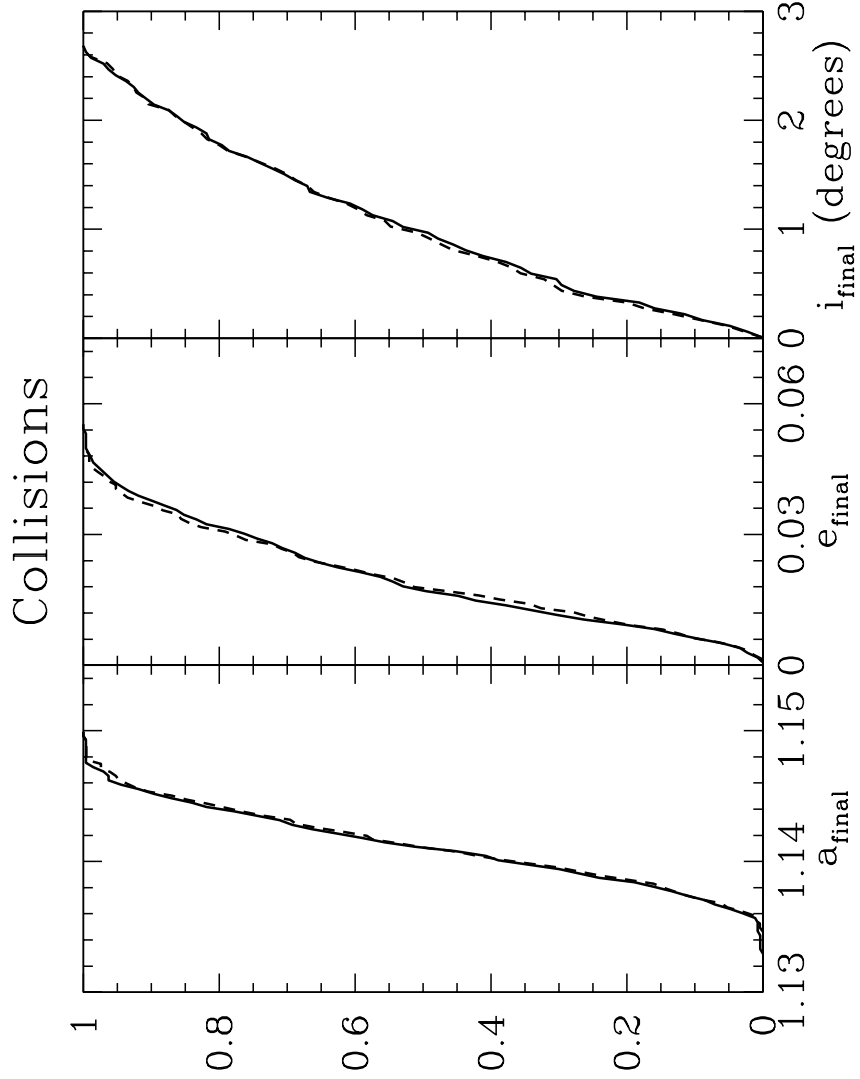


Fig. 8.— Cumulative distributions of the final semimajor axis (left), eccentricity (center), and inclination (right; measured with respect to the initial orbital plane of the inner planet) of the single planet remaining after a collision (assumed to conserve mass and momentum). The solid and dashed lines are for different planetary radii, with $(R/a_1) \times (5 \text{ AU}/R_J) = 5$ and 3, respectively. All planets resulting from a collision have very small eccentricities ($e_{\text{final}} \lesssim 0.05$) and very small inclinations (less than a few degrees). The final semimajor axis is intermediate between the two initial semimajor axes (recall that $a_1 = 1$ and $a_2 \simeq 1.3$ in our units).

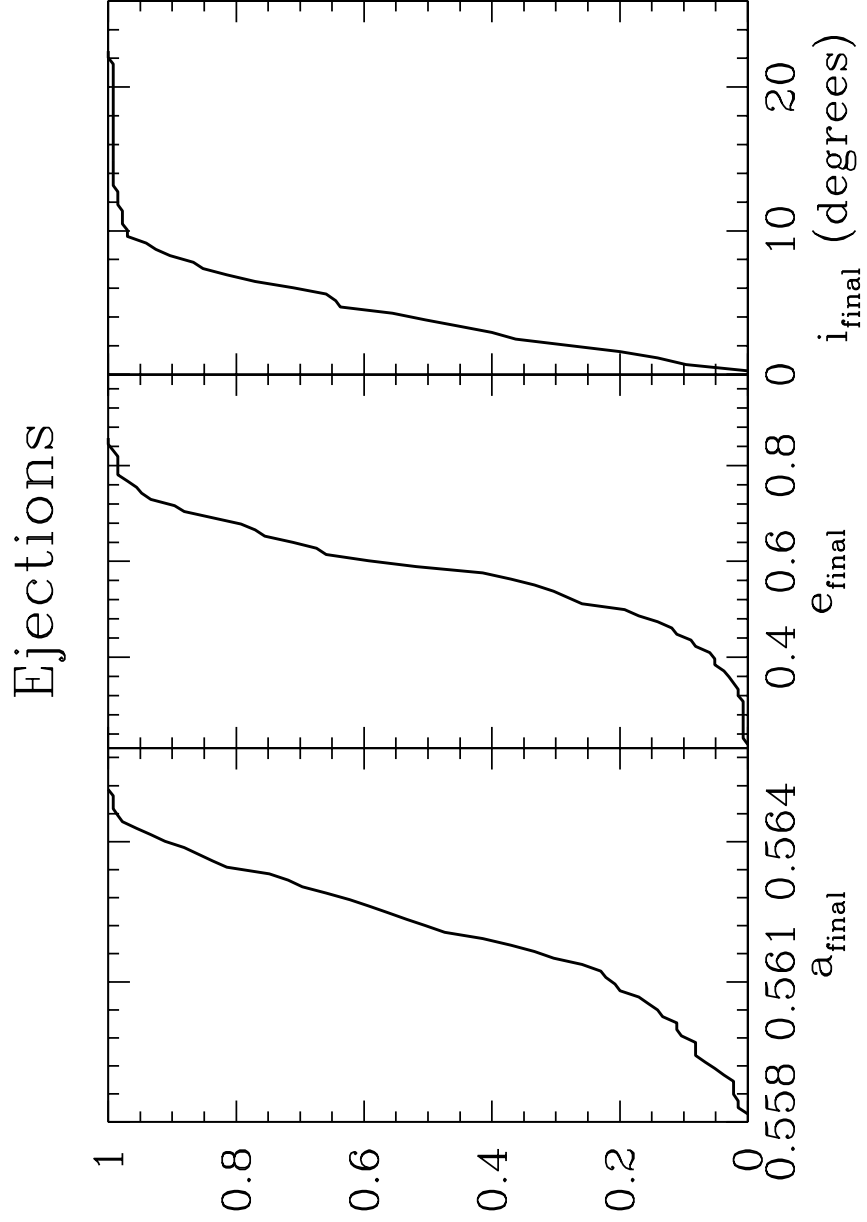


Fig. 9.— Cumulative distributions of the final semimajor axis, eccentricity, and inclination of the remaining planet following ejection of the other. Since the number of ejections is almost independent of planetary radius (see Fig. 7), we only show results for $(R/a_1) \times (5 \text{ AU}/R_J) = 5$.

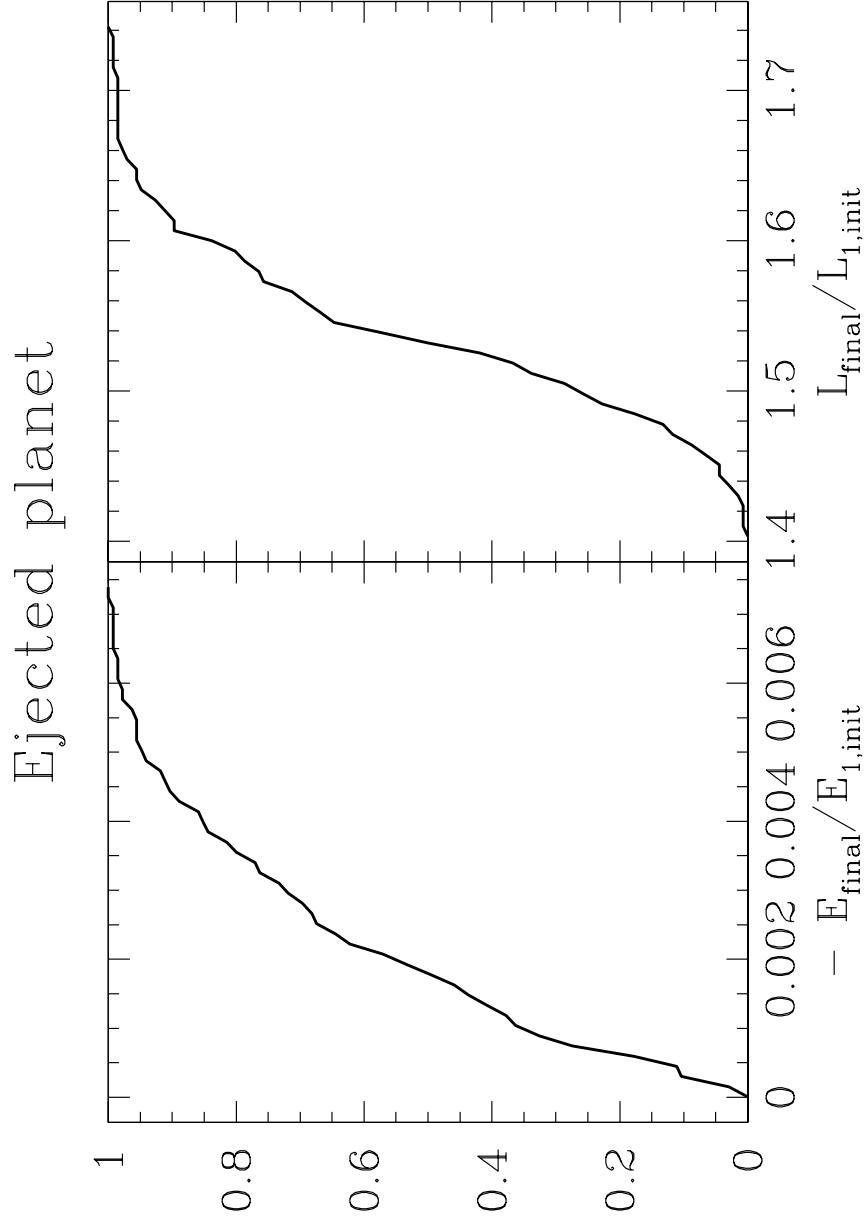


Fig. 10.— Cumulative distributions of the energy and angular momentum of the escaping planet in units of their initial values. While the ejected planet carries very little (positive) energy, it removes a significant amount of angular momentum from the system.

central star. These systems were not included in Figs. 2–9, since the numerical integrations did not conserve energy and angular momentum to the required precision. However a more careful analysis of these systems reveals that the errors accumulated once their orbit already took them very close to the star (at pericenter distances $r_p \lesssim 0.05$). Depending on the initial separation and the radius of the star, these systems could be affected by strong tidal forces that are not included in our simulations. In particular, the orbits could circularize at a very small semimajor axis $a \simeq 2r_p$, or the inner planet could be tidally disrupted by the star.

Finally, we study the properties of systems that are still containing two bound planets at the end of the numerical integrations. The distributions of orbital elements for the inner and outer planets (as determined at the end of the integration), are shown in Fig. 11 and Fig. 12, respectively. These systems can be clearly divided into two categories (see also Fig. 13). About 10% have a large ratio of semimajor axes $a_{\text{outer}}/a_{\text{inner}} \gtrsim 3$ and are either in a stable hierarchical triple configuration, or on their way to the ejection of the outer planet on a timescale exceeding the length of our integrations (recall that we stop integrating after a time $t_{\text{max}} = 2 \times 10^7 \text{ yr } [P_1/12 \text{ yr}]$). Note that the secular evolution of hierarchical triple systems can take place on extremely long timescales that are difficult to probe with direct numerical integrations of the orbital dynamics (see, e.g., Ford *et al.* 2000). Most systems, however (90%), retain a ratio of semimajor axes very close to the initial value. These systems also retain their very small initial eccentricities and inclinations. They clearly represent the dynamically stable region of our initial parameter space. Closer inspection of their properties reveal that they are in fact locked in a nonlinear resonant configuration (see, e.g., Peale 1976) with a near 3:2 ratio of orbital periods, and pericenters that remain anti-aligned at all times (Fig. 14). We will not discuss these systems further in this paper, since their evolution will depend crucially on the dissipation processes that are still at work when the resonant configuration is formed.

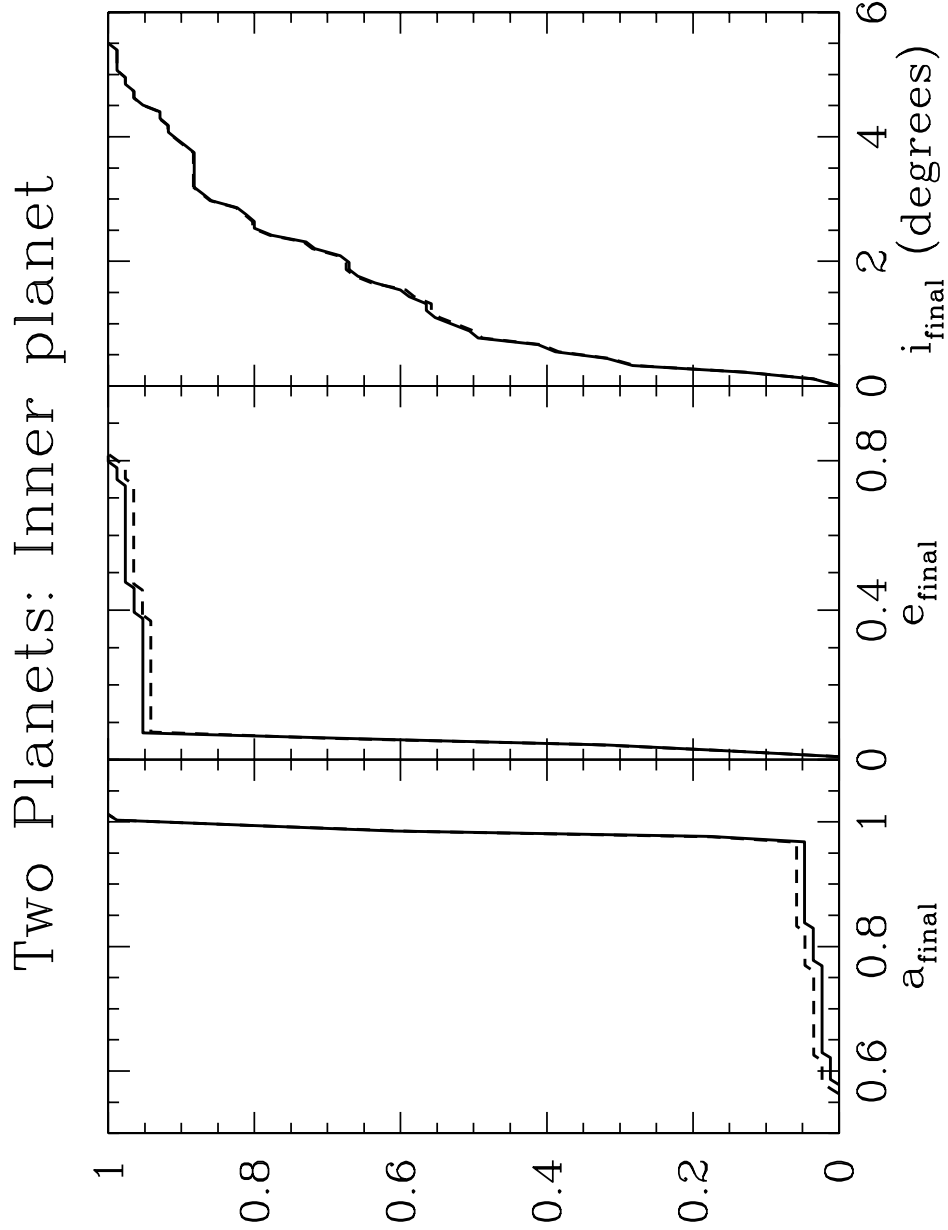


Fig. 11.— Cumulative distributions of the final pericenter separation, eccentricity, and inclination of the inner planet in systems that have retained two bound planets by the end of the numerical integration. The solid and dashed lines are for different planetary radii, with $(R/a_1) \times (5 \text{ AU}/R_J) = 5$ and 1, respectively.

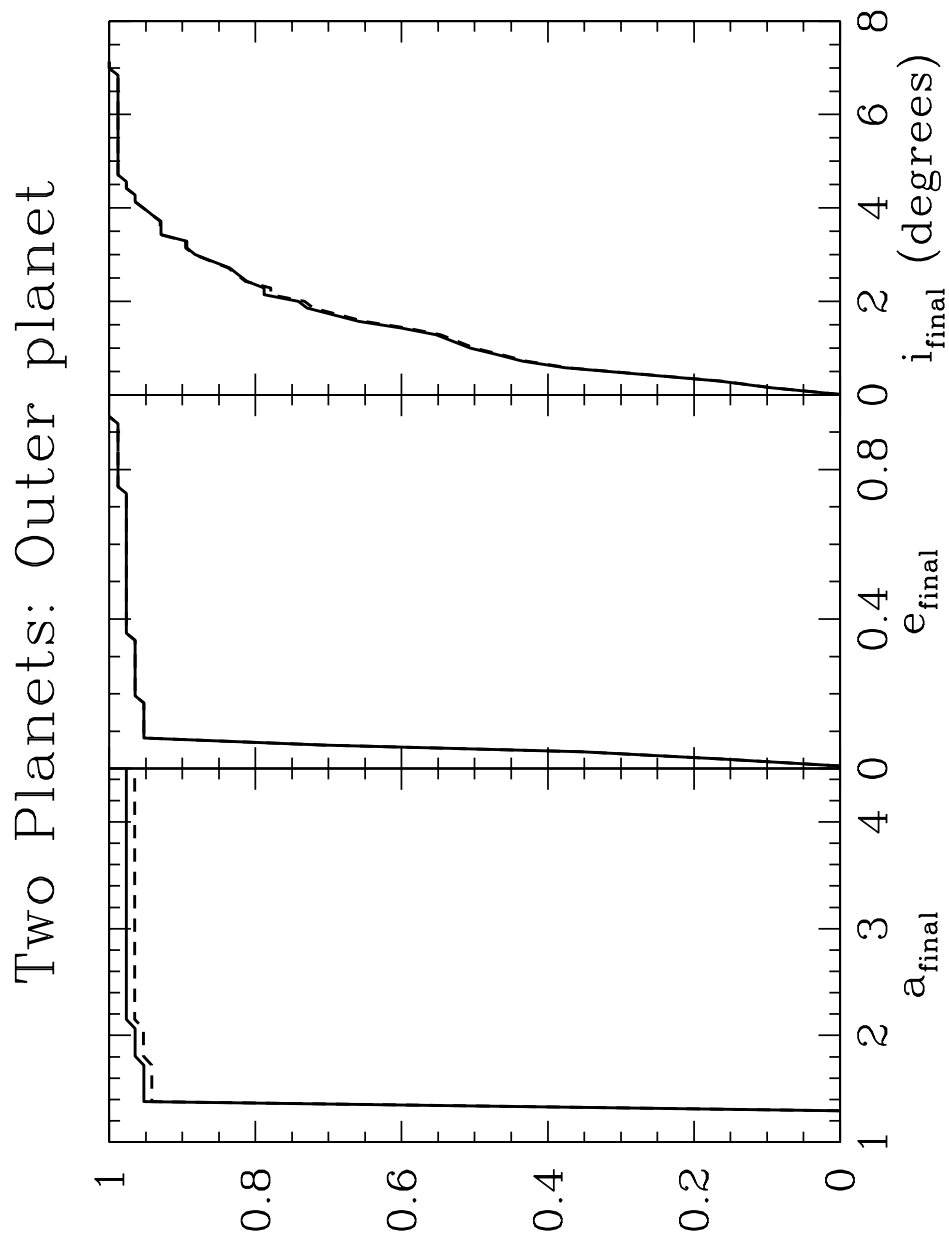


Fig. 12.— Same as Fig. 11 but for the outer planet.

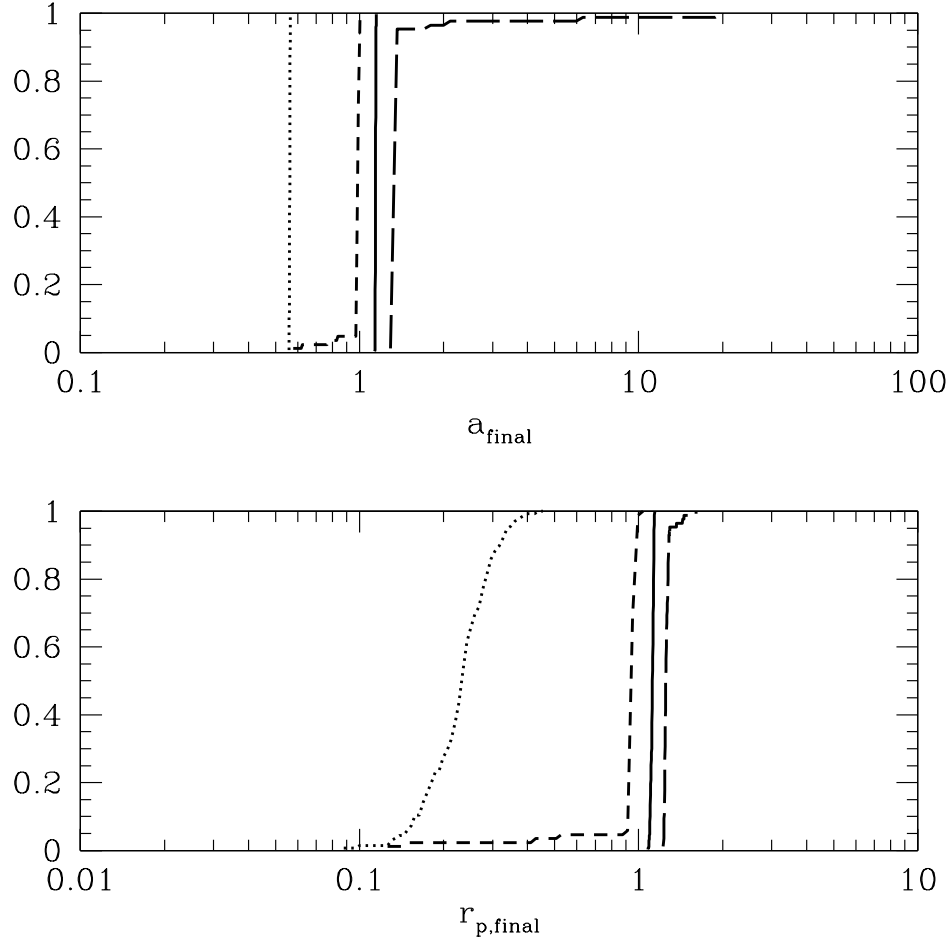


Fig. 13.— Final distributions of semimajor axes and pericenter distances compared for different outcomes. The solid line is for collisions, the dotted line for ejections, and the two dashed lines for systems with both planets remaining. When only one planet remains, conservation of energy dictates a narrow range of semimajor axes. Among systems with two planets remaining, a small fraction may still be on their way to dissociation, while most are in a quasi-stable state.

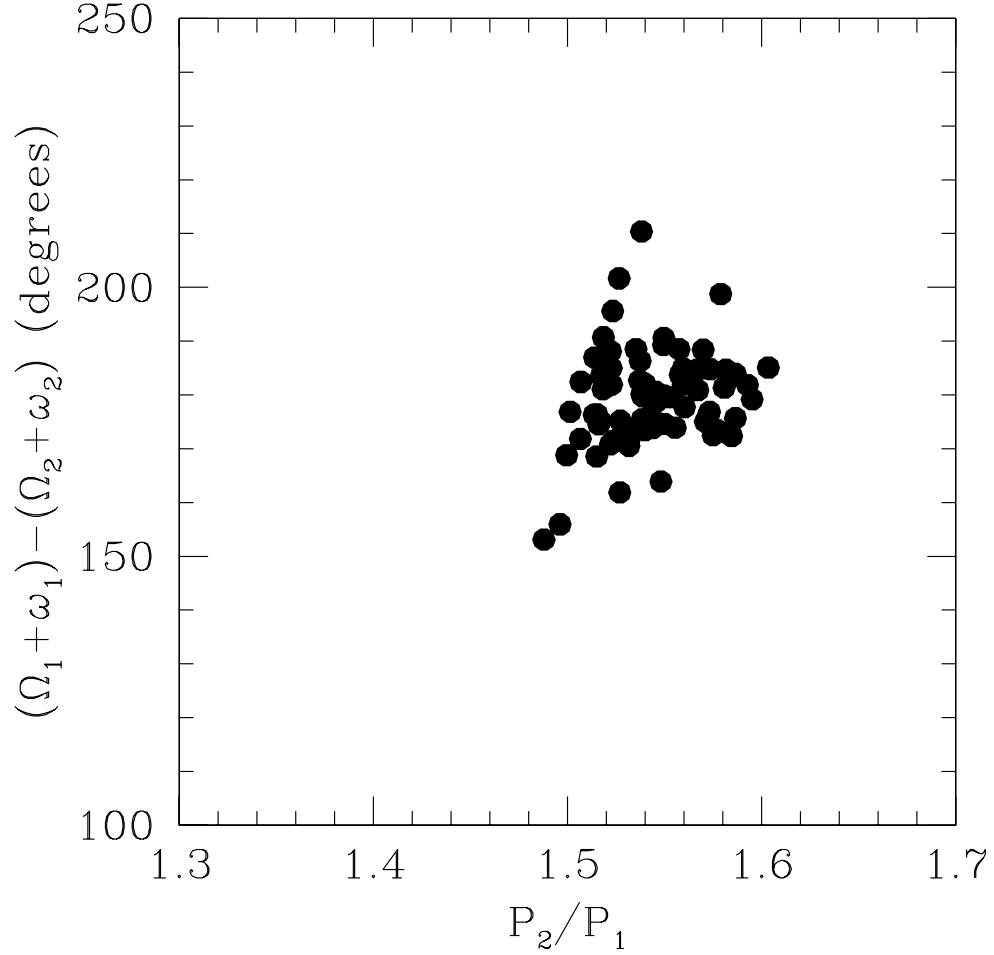


Fig. 14.— Angle between pericenters vs ratio of orbital periods for the two planets when they have remained in a stable, closely coupled configuration until the end of the numerical integration (here ω_1 and ω_2 are the longitudes of pericenters with respect to the ascending nodes, while Ω_1 and Ω_2 are the longitudes of the ascending nodes; subscripts 1 and 2 refer to the inner and outer planets, respectively). The orbits are clearly locked in a nonlinear 3:2 resonance.

4. Comparison with Observations

The known extrasolar planets (Fig. 1) can be roughly divided into two groups: those with short-period, nearly circular orbits ($a \lesssim 0.07$ AU) and those with wider and more eccentric orbits ($a \gtrsim 0.07$ AU).

Many of the short-period planets, like their prototype 51 Peg, are so close to their parent star that tidal dissipation would have likely circularized their orbits, even if they were originally eccentric (Rasio *et al.* 1996). Thus, their small observed eccentricities do not provide a good indicator of their dynamical history. Circularization of extremely eccentric orbits produced by dynamical instabilities (as originally proposed by Rasio and Ford 1996) seems unlikely to be the dominant mechanism for producing these systems. Indeed, the observed frequency of 51 Peg type systems appears much higher than would be predicted by such a dynamical scenario: in the observed sample the frequency is $\sim 20\%$, while among all stars searched for planetary-mass companions it is $\sim 1\%$ (Marcy and Butler 2000). In contrast, on the basis of our simulations for two planets, we would estimate that at most a few in $\sim 10^3$ systems affected by dynamical instabilities would produce an orbit eccentric enough to be circularized by tidal dissipation at $r \lesssim 0.07$ AU. We note, however, that tidal interaction with a (much larger) pre-main-sequence star, or dissipation in a gaseous disk, could circularize orbits at a considerably larger distance from the star, increasing the predicted frequency of circularized systems in our scenario (see Fig. 13). Observational support for the existence of a circularization mechanism operating at distances as large as $r \sim 0.2$ AU is provided by some of the wider systems with nearly circular orbits, such as ρ CrB (with $a \simeq 0.23$ AU and $e < 0.07$; see Noyes *et al.* 1997). These orbits are clearly too wide to have been circularized by tidal dissipation in the star or in the planet, according to the standard theory (Ford *et al.* 1999). We note also that the observation of a single giant planet on a nearly circular orbit does *not* imply that the parent planetary system must have

been dynamically stable, since a frequent outcome of a dynamical instability is a collision between two planets, which leaves a more massive single planet on a nearly circular orbit (assuming the initial orbits of the two planets were nearly circular; see Fig. 8).

The large eccentricities of most planets with longer periods also require an explanation. A planet that would have formed from a protoplanetary disk in the standard manner is unlikely to have developed such a large eccentricity, since dissipation in the disk tends to circularize orbits. Dynamical instabilities leading to the ejection of one planet while retaining another planet of comparable mass can naturally explain the observed distribution of eccentricities. A direct comparison between the observations and our results (Fig. 15) suggests that dynamical instabilities would actually tend to *overproduce* highly eccentric orbits. However, since our simulations were done for two *equal-mass* planets, they provide an *upper limit* to the actual distribution. Indeed, for slightly unequal masses, the dynamical interactions will tend to eject preferentially the less massive planet, thereby allowing the more massive planet to retain a higher angular momentum. We can see easily that only a small departure from the equal-mass case would be necessary to bring our predicted eccentricity distribution in closer agreement with the observed one. The median eccentricity in the observed sample is about 0.3, while it is about 0.6 in our simulations. To reduce the eccentricity from 0.6 to 0.3 for the retained planet corresponds to an increase in orbital angular momentum by a factor $(1 - 0.3^2)^{1/2} / (1 - 0.6^2)^{1/2} \simeq 1.2$. Thus a $\sim 20\%$ reduction in the angular momentum removed by the escaping planet, which could be achieved by a $\sim 20\%$ reduction in its mass, would be sufficient to bring our results in close agreement with the observed distribution.

Our scenario also imposes tight constraints on the distribution of semimajor axes that are far more difficult to reconcile with observations. What is perhaps most striking about the orbital parameters of the observed systems with $a \gtrsim 0.07$ AU in Fig. 1 is the paucity

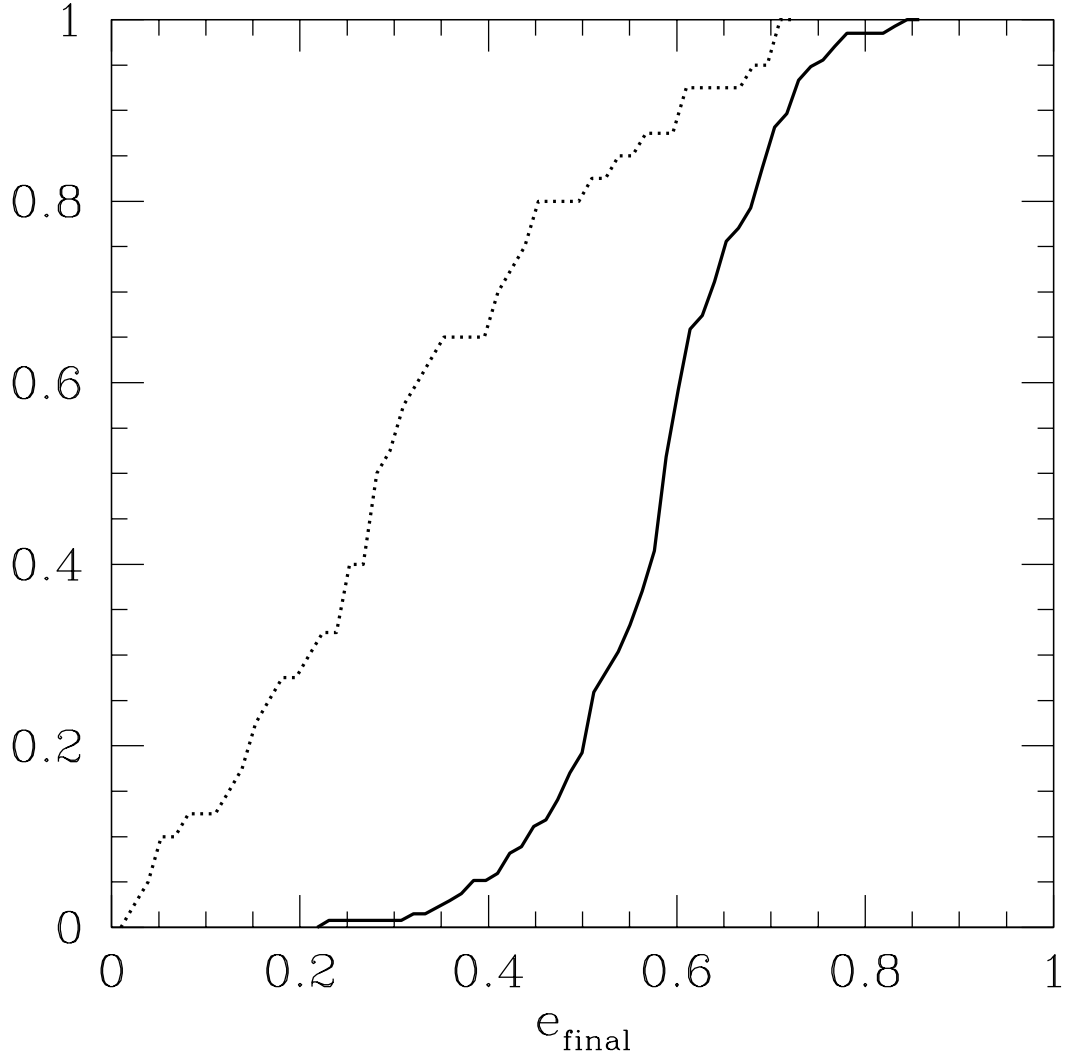


Fig. 15.— Cumulative distribution of orbital eccentricities for the observed systems (dotted line; we included all orbits with $a > 0.07$ AU in Fig. 1), compared to the eccentricity distribution predicted by our numerical simulations for the remaining planet following an ejection (solid line, as in Fig. 9). The median eccentricity of the observed sample is about 0.3, compared to 0.6 from the simulations.

of circular orbits. However, in our scenario, we cannot avoid a certain fraction of systems that still contain a giant planet on a nearly circular orbit, following a collision between the two initial planets. From Fig. 7 we see that, to avoid a significant fraction of collisions, we must have $(R/R_J)/(a_1/5 \text{ AU}) \lesssim 1$. Since $a_f \simeq 0.56a_1$ for the retained planet following an ejection, we deduce that, if most of the observed planets on wide eccentric orbits had been retained following the ejection of another planet (and with most avoiding a collision), their semimajor axes should satisfy $a_f \gtrsim 2.5 \text{ AU} (R/R_J)$. Instead, in the range of semimajor axes observed for eccentric systems, $a \simeq 0.07 - 3 \text{ AU}$, we would expect that collisions would be about ~ 3 times more frequent than ejections, implying that the fraction of highly eccentric orbits could not exceed $\sim 1/4$ of the observed systems. Reducing the planetary radius to $R \simeq 0.1 R_J$ would provide very good agreement with observations (and collisions would then explain nicely the existence of systems like $\rho \text{ CrB}$), but this seems rather implausible: even a giant terrestrial (rocky) planet with $m \gtrsim 0.5 M_J$ would have $R \simeq 0.3 R_J$ (Guillot *et al.* 1996). Moreover, we note that the observations of transits indicate that HD 209458b must be a hydrogen-rich gas giant (Burrows *et al.* 2000).

We are grateful to Scott Tremaine for valuable conversations. We also thank the referees, S. Ida and P. Wiegert, for many useful comments on the original manuscript. This work was supported in part by NSF Grant AST-9618116 and NASA ATP Grant NAG5-8460. F.A.R. was supported in part by an Alfred P. Sloan Research Fellowship. Our computations were supported by the National Computational Science Alliance under Grant AST980014N and utilized the SGI/Cray Origin2000 supercomputers at Boston University and NCSA, and the Condor system at the University of Wisconsin.

REFERENCES

- Armitage, P.J., and B.M.S. Hansen 1999. Early planet formation as a trigger for further planet formation. *Nature* **402**, 633–635.
- Beckwith, S.V.W., & Sargent, A.I. 1996, Circumstellar disks and the search for neighboring planetary systems. *Nature* **383**, 139–144.
- Bodenheimer, P., O. Hubickyj, and J.J. Lissauer 2000. Models of the in Situ Formation of Detected Extrasolar Giant Planets. *Icarus* **143**, 2–14.
- Boss, A.P. 1995. Proximity of Jupiter-Like Planets to Low-Mass Stars. *Science* **267**, 360–363.
- Boss, A.P. 1996. Forming a Jupiter-like Companion for 51 Pegasi. *Lunar & Planetary Science* **27**, 139–140.
- Boss, A.P. 1998. Evolution of the Solar Nebula. IV. Giant Gaseous Protoplanet Formation. *Astrophys. J.* **503**, 923–937.
- Burrows, A., T. Guillot, W.B. Hubbard, M.S. Marley, D. Saumon, J.I. Lunine, and D. Sudarsky 2000. On the Radii of Close-in Giant Planets. *ApJ* **534**, L97–L100.
- Burrows, A., M. Marley, W.B. Hubbard, J.I. Lunine, T. Guillot, D. Saumon, R. Freedman, D. Sudarsky, and C. Sharp 1997. A Nongray Theory of Extrasolar Giant Planets and Brown Dwarfs. *ApJ* **491**, 856–875.
- Butler, R.P., G.W. Marcy, D.A. Fischer, T.M. Brown, A.R. Contos, S.G. Korzennik, P. Nisenson, and R.W. Noyes 1999. Evidence for Multiple Companions to Upsilon Andromedae. *ApJ* **526**, 916–927.
- Chambers, J.E., G.W. Wetherill, and A.P. Boss 1996. The Stability of Multi-Planet Systems. *Icarus* **119**, 261–268.

- Charbonneau, D., T.M. Brown, D.W. Latham, and M. Mayor 2000. Detection of Planetary Transits Across a Sun-like Star. *ApJ* **529**, L45–L48.
- Duncan, M.J., and T. Quinn 1993. The long-term dynamical evolution of the solar system. *Ann. Rev. Astron. Astrophys.* **31**, 265–295.
- Ford, E.B., B. Kozinsky, and F.A. Rasio 2000. Secular Evolution of Hierarchical Triple Star Systems. *ApJ* **535**, 385–401.
- Ford, E.B., F.A. Rasio, and A. Sills 1999. Structure and Evolution of Nearby Stars with Planets. I. Short-Period Systems. *ApJ* **514**, 411–429.
- Fridlund, C.V.M. 1999. The Infrared Space Interferometer DARWIN. American Astronomical Society, DPS meeting No. 31, paper 29.04.
- Gaudi, B.S. *et al.* 2000. Microlensing Constraints on the Frequency of Jupiter Mass Planets. To appear in *Microlensing 2000: A New Era of Microlensing Astrophysics*, ASP Conf. Series, eds. J.W. Menzies and P.D. Sackett.
- Gladman, B. 1993. Dynamics of systems of two close planets. *Icarus* **106**, 247–258.
- Goldreich, P., and S. Tremaine 1980. Disk-satellite interactions. *ApJ* **241**, 425–441.
- Guillot, T., A. Burrows, W.B. Hubbard, J.I. Lunine, and D. Saumon 1996. Giant Planets at Small Orbital Distances. *ApJ* **459**, L35–L38.
- Hatzes, A.P. *et al.* 2000. Evidence for a Long-period Planet Orbiting Epsilon Eridani. To appear in *ApJ Letters* [astro-ph/0009423].
- Henry, G.W., G.W. Marcy, R.P. Butler, and S.S. Vogt 2000. A Transiting “51 Peg-like” Planet. *ApJ* **529**, L41–L45.

- Holman, M., J. Touma, and S. Tremaine 1997. Chaotic variations in the eccentricity of the planet orbiting 16 CYG B. *Nature* **386**, 254–256.
- Innanen, K.A., J.Q. Zheng, S. Mikkola, and M.J. Valtonen 1997. The Kozai Mechanism and the Stability of Planetary Orbits in Binary Star Systems. *AJ* **113**, 1915–1927.
- Katz, J.I. 1997. Single Close Encounters Do Not Make Eccentric Planetary Orbits. *ApJ* **484**, 862–865.
- Kley, W. 2000. On the migration of a system of protoplanets. *MNRAS* **313**, L47–L51.
- Korzennik, S.G., T.M. Brown, D.A. Fischer, P. Nisenson, and R.W. Noyes 2000. A High-Eccentricity Low-Mass Companion to HD 89744. *ApJ* **533**, L147–L150.
- Levison, H.F., and M.J. Duncan 1994. The long-term dynamical behavior of short-period comets. *Icarus* **108**, 18–36.
- Lin, D.N.C, and S. Ida 1997. On the Origin of Massive Eccentric Planets. *ApJ* **447**, 781–791.
- Lin, D.N.C., P. Bodenheimer, and D.C. Richardson 1996. Orbital migration of the planetary companion of 51 Pegasi to its present location. *Nature* **380**, 606–607.
- Lissauer, J.J. 1993. Planet formation. *ARAA* **31**, 129–174.
- Lombardi, J.C., Jr., F.A. Rasio, and S.L. Shapiro 1996. Collisions of Main-Sequence Stars and the Formation of Blue Stragglers in Globular Clusters. *ApJ* **468**, 797–818.
- Malhotra, R. 1995. The Origin of Pluto’s Orbit: Implications for the Solar System Beyond Neptune. *AJ* **110**, 420–429.
- Marcy, G.W., and R.P. Butler 1998. Detection of Extrasolar Giant Planets. *Ann. Rev. Astron. Astrophys.* **36**, 57–98.

- Marcy, G.W., and R.P. Butler 2000. Planets Orbiting Other Suns. *PASP* **112**, 137–140.
- Marcy, G.W., R.P. Butler, and S.S. Vogt 2000. Sub-Saturn Planet Candidates to HD 16141 and HD 46375. To appear in *ApJ* [astro-ph/0004326].
- Marzari, F., and S.J. Weidenschilling 1999. On the Eccentricities of Extrasolar Planets. *AAS*, DPS meeting 31, paper 05.07.
- Mazeh, T., Y. Krymolowski, and G. Rosenfeld 1997. The High Eccentricity of the Planet Orbiting 16 Cygni B. *ApJ* **477**, L103–L106.
- Mazeh, T., S. Zucker, A. dalla Torre, and F. van Leeuwen 1999. Analysis of the HIPPARCOS Measurements of upsilon Andromedae: A Mass Estimate of Its Outermost Known Planetary Companion. *ApJ* **522**, L149–L151.
- Murray, N., B. Hansen, M. Holman, and S. Tremaine 1998. Migrating Planets. *Science* **279**, 69–71.
- Nelson, R.P., J. Papaloizou, F. Masset, and W. Kley 2000. Numerical Simulations of Disc-Companion Interactions: Implications for Extrasolar Giant Planets. To appear in *Planetary Systems in the Universe* (IAU Symp. 202).
- Noyes, R.W., S. Jha, S.G. Korzennik, M. Krockenberger, P. Nisenson, T.M. Brown, E.J. Kennelly, and S.D. Horner 1997. A Planet Orbiting the Star Rho Coronae Borealis. *ApJ* **483**, L111–L114; erratum **487**, L195.
- Papaloizou, J.C.B. 2000. Orbital parameters of extra-solar planets. To appear in *Planetary Systems in the Universe* (IAU Symp. 202).
- Peale, S.J. 1976. Orbital resonances in the solar system. *Ann. Rev. Astron. Astrophys.* **14**, 215–246.

- Perryman, M.A.C. 2000. Extra-Solar Planets. To appear in *Inst. of Physics, Reports on Progress in Physics* [astro-ph/0005602].
- Rasio, F.A., and E.B. Ford 1996. Dynamical instabilities and the formation of extrasolar planetary systems. *Science* **274**, 954–956.
- Rasio, F.A., C.A. Tout, S.H. Lubow, and M. Livio 1996. Tidal Decay of Close Planetary Orbits. *ApJ* **470**, 1187–1191.
- Rivera, E.J., and J.J. Lissauer 2000. Stability Analysis of the Planetary System Orbiting ν Andromedae. *ApJ* **530**, 454–463.
- Santos, N.C., M. Mayor, D. Naef, F. Pepe, D. Queloz, S. Udry, M. Burnet, and Y. Revaz 2000. The CORALIE survey for Southern extra-solar planets. III. A giant planet in orbit around HD 192263. *Astron. Astrophys.* **356**, 599–602.
- Trilling, D.E., W. Benz, T. Guillot, J.I. Lunine, W.B. Hubbard, and A. Burrows 1998. Orbital Evolution and Migration of Giant Planets: Modeling Extrasolar Planets. *ApJ* **500**, 428–439.
- Vogt, S.S., G.W. Marcy, R.P. Butler, and K. Apps 2000. Six New Planets from the Keck Precision Velocity Survey. To appear in *ApJ*.
- Weidenschilling, S.J., and F. Marzari 1996. Gravitational scattering as a possible origin for giant planets at small stellar distances. *Nature* **384**, 619–620.
- Wisdom, J., and M. Holman 1991. Symplectic maps for the N -body problem. *AJ* **102**, 1528–1539.
- Wisdom, J., and M. Holman 1992. Symplectic maps for the N -body problem — stability analysis. *AJ* **104**, 2022–2029.

Appendix: Simple Analytic Estimates

Here we set $G = 1$, but we retain factors of $a_1 = 1$ and $M = 1$ (in our units) in all equations for clarity.

Collisions

If we could entirely neglect the change in orbital energy following a collision of two planets, under our assumptions that collisions conserve both mass and momentum, the final semimajor axis for the new planet of mass $2m$ would be given by

$$a_f = -\frac{2mM}{2E_f} \simeq -\frac{mM}{(E_1 + E_2)} \simeq \frac{2a_1a_2}{a_1 + a_2}, \quad (1)$$

where a_1 and a_2 are the initial semimajor axes of the two planets (E_f is the final orbital energy, E_1 and E_2 the initial orbital energies of the two planets, and we have neglected the interaction energy, which represents a fractional error $\sim m/M \sim 10^{-3}$). The resulting range of a_f/a_1 (taking into account our small range of initial values for a_2/a_1) is $\simeq 1.12 - 1.13$. This is slightly *lower* than the actual range obtained from our simulations, where $a_f/a_1 \simeq 1.13 - 1.15$ (see Fig. 8), indicating that the total orbital energy of the system *increases* by about 1 – 2% following a collision.

We can easily understand this result by considering the following simple model for a collision, suggested by our numerical results (see Fig. 3). As long as they are well outside each other’s sphere of influence (where the mutual gravitational attraction of the two planets becomes dominant over the central star), the relative velocity between the two planets remains always very small compared to the escape speed from their surface. Indeed, the relative velocity is $v_r \sim 0.5(M/a^3)^{1/2} \Delta a$ for two planets separated by $\Delta a = a_2 - a_1$,

This manuscript was prepared with the AAS L^AT_EX macros v5.0.

while the escape speed $v_e = (2m/R)^{1/2}$, giving

$$\frac{v_r}{v_e} \sim 3 \times 10^{-2} \left(\frac{M/m}{10^3} \right)^{1/2} \left(\frac{R/a}{10^{-4}} \right)^{1/2} \left(\frac{\Delta a/a}{0.3} \right). \quad (2)$$

The radius r_i of the sphere of influence is determined by setting $m^2/r_i^2 \sim Mm/a^2$, giving $r_i \sim (m/M)^{1/2} a \gg R$. In the center-of-mass frame of the two planets, the collision resembles a head-on collision between two planets of mass m starting from a distance r_i at rest. Neglecting $(v_r/v_e)^2 \ll 1$, we see that the orbital energy change following the collision (which leaves a single planet of mass $2m$ at rest in the center-of-mass frame) is equal to the gravitational binding energy m^2/r_i . The fractional increase in the total orbital energy following a collision should therefore be $\Delta E/E \sim (m^2/r_i)/(2Mm/a) \sim 0.5 (m/M)^{1/2}$, which is $\sim 1.5\%$ for $m/M = 10^{-3}$, in close agreement with the numerical results. Note that this argument is completely independent of the details of the collision itself, which converts a much larger amount of kinetic energy into heat through shocks, and a much larger amount of gravitational binding energy of the two planets just before impact into binding energy of the collision product.

Having determined the final semimajor axis following a collision, we can now also estimate the final eccentricity from conservation of angular momentum. With obvious notations we write, for two nearly circular and coplanar initial orbits,

$$L_f = \frac{2mM}{M+2m} \sqrt{(M+2m)a_f(1-e_f^2)} \quad (3)$$

$$= L_1 + L_2 \quad (4)$$

$$= \frac{mM}{M+m} \left(\sqrt{(M+m)a_1} + \sqrt{(M+m)a_2} \right), \quad (5)$$

and solving for the final eccentricity gives

$$1 - e_f^2 = \frac{(M+2m) (\sqrt{a_1} + \sqrt{a_2})^2}{4a_f(M+m)}. \quad (6)$$

The *maximum* final eccentricity is obtained by minimizing the RHS. For $m/M = 10^{-3}$, $a_1 = 1$, $a_2 = 1.3$, and $a_f = 1.15$ (the maximum value of a_f , taking into account the slight

increase in orbital energy estimated above; see Fig. 8), we obtain $e_f < 0.05$, in perfect agreement with our numerical results (see Fig. 8).

Ejections

Similarly we can try to predict the orbital properties of the remaining planet following an ejection. Since the ejected planet leaves the system on a very nearly-parabolic orbit, we can estimate the final semimajor axis of the retained planet from energy conservation,

$$a_f = -\frac{mM}{2E_f} \simeq -\frac{mM}{2(E_1 + E_2)} \simeq \frac{a_1 a_2}{a_1 + a_2}, \quad (7)$$

using the same notations and assumptions as above. With $a_1 = 1$ and $a_2 = 1.3$ we obtain $a_f \simeq 0.565$, which is precisely the upper limit of the range of values, $a_f \simeq 0.558 - 0.565$, obtained from our simulations (Fig. 9). Thus the (positive) energy carried away by the escaping planet is at most $\simeq 0.7\%$ of its initial binding energy (in agreement with the distribution of escaping energies shown in Fig. 10).

We can again try to estimate the final eccentricity using conservation of angular momentum. With the same notations as before and with r_{pe} denoting the pericenter distance of the ejected planet's parabolic orbit we have

$$L_f = \frac{mM}{M+m} \left(\sqrt{(M+m)a_f(1-e_f^2)} + \sqrt{2(M+m)r_{pe}} \right) \quad (8)$$

$$= L_1 + L_2 \quad (9)$$

$$= \frac{mM}{M+m} \left(\sqrt{(M+m)a_1} + \sqrt{(M+m)a_2} \right). \quad (10)$$

Solving for the final eccentricity and using eq. (7) gives

$$1 - e_f^2 \simeq \frac{a_1 + a_2}{a_1 a_2} \left(\sqrt{a_1} + \sqrt{a_2} - \sqrt{2r_{pe}} \right)^2. \quad (11)$$

Unfortunately no simple argument can be used to predict precise values of r_{pe} . Clearly, however, we expect the pericenter distance r_{pe} of the ejected planet to be just slightly larger

than the apocenter distance of the inner (retained) planet, i.e., $r_{pe} \gtrsim 1$. From the range of values of the final eccentricity $e_f \simeq 0.4 - 0.8$ observed in our simulations (Fig. 9), we deduce that $r_{pe} \simeq 1 - 1.4$.

In this section we wish to predict what the final orbital elements for ejections and collisions should be, using analytic methods, and compare them to the actual results of our simulations.

1 Notation and basic formulas

In the following sections we shall use notation as follows:

a - semimajor axis e - eccentricity E - energy L - angular momentum m - mass of either planet M - mass of the star

The subscripts i and f will stand for initial and final parameters, respectively. Subscripts 1 and 2 will stand for the parameters referring to the initially inner and outer planet, in that order.

The basic formula for energy and angular momentum of an orbit is then

$$E = -\frac{m}{2a} \quad L = \frac{Mm}{M+m} \sqrt{G(M+m)a(1-e^2)} \quad (1)$$

2 Collisions

Assuming a complete conservation of energy, we can estimate the final semi-major axis of the planet resulting from a collision:

$$a_f = -\frac{2m}{2E_f} = -\frac{m}{(E_1 + E_2)} = \frac{2a_1a_2}{a_1 + a_2} \quad (2)$$

The resulting range of a_f (taking into account our distribution of initial orbital elements) is approx. $1.123 - 1.13$, which is slightly lower than the actual range resulting from our simulation. This is a consequence of our energy conservation assumption, which is not very accurate for an inelastic collision. We can easily estimate the actual amount of dissipated energy:

$$\frac{E_{actual}}{E_1 + E_2} = \frac{a_{f,calculated}}{a_{f,actual}} \quad (3)$$

The resulting dissipation is between 1 and 2%.

We can also estimate the final eccentricity, assuming conservation of angular momentum in the z direction (which, given the small inclinations, is approximately equal to its total magnitude):

$$\begin{aligned} L_f &= L_1 + L_2 \\ \frac{2mM}{M+2m}\sqrt{(M+2m)a_f(1-e_f^2)} &= \frac{mM}{M+m}\left(\sqrt{(M+m)a_1(1-e_1^2)} + \sqrt{(M+m)a_2(1-e_2^2)}\right) \end{aligned} \quad (4)$$

which gives us the formula

$$e_f = \sqrt{1 - \frac{(M+2m)\left(\sqrt{a_1(1-e_1^2)} + \sqrt{a_2(1-e_2^2)}\right)^2}{4a_f(M+m)}} \quad (6)$$

$$(7)$$

This means that e_f is in the range of approximately $\sqrt{1 - \frac{1.126}{a_f}}$ to $\sqrt{1 - \frac{1.147}{a_f}}$.

Since the expression under the square root has to be non-negative, we can use this equation to estimate the semimajor axis (assuming the final eccentricity to be 0), to be in the range of $1.126 - 1.147$, which matches the data a little better; more than 95% of the outcomes are under 1.147. The lower bound of 1.126 is slightly lower than the result of our simulations, which has a lower bound of about 1.135. We can use this to estimate the dissipation of energy again, getting a result of about 1%.

EXPLANATION OF THIS? I HAVE NO IDEA.

3 Ejections

Ejections are a little harder to predict exactly, since we cannot know how much energy the escaping planet is carrying away. Assuming it carries none, we can get the highest possible final semimajor axis of the remaining planet:

$$a_f = -\frac{m}{2E_f} = -\frac{m}{2(E_1 + E_2)} = \frac{a_1 a_2}{a_1 + a_2} \quad (8)$$

which gives the maximum of 0.565, consistently with our simulation results.

From conservation of angular momentum, we can get the following:

$$e_f = \sqrt{1 - \frac{L_f^2(1+m)}{a_f m^2}} = \sqrt{1 - \frac{L_f^2(1+m)(a_1 + a_2)}{a_1 a_2 m^2}} \quad (9)$$

Setting the final eccentricity to be 0, we can get the maximal angular momentum left to the bound planet to be about 0.75 in the units of $L_{1,init}$, the initial angular momentum of the inner planet. That sets the angular momentum carried away by the escaping planet to be in the range of 1.38-2.14 $L_{1,init}$